 DOI: 10.1002/masy.200851416

Experimental Observations and Quantitative Predictions of Rheological Properties of Organoclay/Poly(propylene) Nanocomposites at the Startup of Shear Flows

Mahmoud Rajabian, Ghasem Naderi*

Summary: We study the rheological characteristics of nanocomposites containing nano-sized plate like particles in a viscoelastic fluid at the startup of steady state in the simple shear flow mode. The nanocomposites of organoclay-polypropylene with different nanoclay contents were prepared by melt mixing. A rheological equation of state, originally formulated to predict the orientation state and viscoelastic behavior of suspensions of ellipsoidal particles in polymer melts, has been modified to describe the observed phenomena for the nanoclay/poly(propylene) composites. The rotational particle motion and alignment for a group of symmetric ellipsoids with the applied flow field are investigated. Additionally, model calculations of the macroscopic rheological properties for a simple flow case suggest the presence of nano-particles significantly modify the suspended fluid at volume concentrations as low as 0.5%. The model calculations for the startup viscosity are reasonably in agreement with the experimental results at the experimental range covered in this study. At the shear rate of $\dot{\gamma} = 1\ s^{-1}$, we observe pronounced stress overshoots at the three nanoclay loadings level tested which are found to be related to the fast alignment of the silicate layers with the shear direction in the polymer melt.

Keywords: modeling; rheology; thermoplastic nanocomposites

Introduction

Recent advances in synthesis, chemical modifications and separation of carbon nano-tubes and nanoclay particles have brought much attention towards development of new techniques to fabrication of nanocomposite materials with the significant improvements in impact and tensile modulus and strength, gas permeability, flammability and resistance against solvents and heat. Because of their important roles in processing and applications involving of nano-filled polymeric systems, suspensions of lamellar particles in viscoelastic fluids are of great practical interest. In all processes involving the lamellar particles, strong shear, elongation or combined flows are applied to the suspension under process and hence strong microscopic structural developments are expected. The changes in microstructure will in turn govern the macroscopic flow properties such as viscous dissipation and elasticity. Furthermore, the macroscopic characteristics of the nanocomposites such as mechanical strength are determined during flow by the state of alignment and interactions of the particles with the polymer matrix and it is highly desirable to predict such properties provided the orientation of particles in the polymer matrix. Those are some of the reasons to undertake a theoretical investigation on the microscopic alignment of thin layered particles dispersed in the viscoelastic fluid phase with particles sizes ranging from 10 nm to 1 micron and aspect ratios (thickness to diameter) down to 1/100 which are similar to those of organically modified

Iran Polymer and Petrochemical Institute IPPI, P.O.Box 149650115, Tehran, Iran
E-mail: m.rajabian@ippi.ac.ir

clays currently used in most polymer nano-composite applications [see e.g. references[1–4]]. The goal of this paper is to present the results of our investigations on orientation kinetics and rheology of the nano-sized clay lamellae/polypropylene suspensions under simple shear flows. This work which indeed is a follow up of our previous research on particulate suspensions in both Newtonian and viscoelastic fluids presents a mesoscopic level modeling for a group of symmetric spheroids in a FENE-P type matrix.[1,2,5,6]

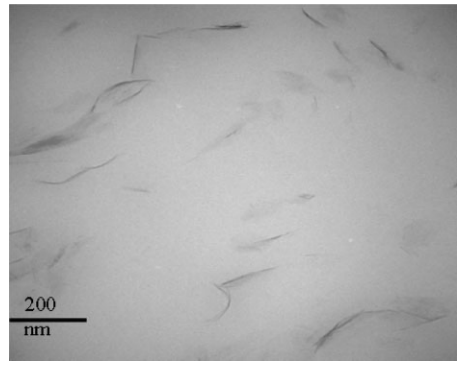

Figure 1.
TEM picture of the organoclay/PP nano-composite; $\phi_v = 0.5\%$.

Experimental Part

The nanocomposites of organoclay/PP at three particle loadings (3, 5, and 7%wt corresponding to 0.5, 1 and 1.5%vol, respectively) were prepared by melt blending in a complex multi-step process described elsewhere[1]. A commercial grade polypropylene (PP, Pro-fax 6523, Tm = 165 °C) with a melt flow index (MFI) of 4 g/10 mn was used as the matrix phase. The clay used was Cloisite 15A from Southern Clay Products, and to render it compatible with the polypropylene matrix, a compatibilizing agent, i.e. the maleic anhydride-modified polypropylene (PPMA, Epolene G3015 from Eastman Chemical) was added with a PPMA/Clay weight ratio of three. The maleic anhydride-modified polypropylene (PPMA) Epolene G3015 (acid number = 15, MA = 1%) was obtained from Eastman Chemical. For all master batches, the PPMA/clay weight ratio was kept constant, i.e. 3:1. Following the mixing process, the particles were found entirely dispersed in the polymer matrix. Further details on materials, preparation and characterization methods can be found in a previous publication. Figure 1 depicts the

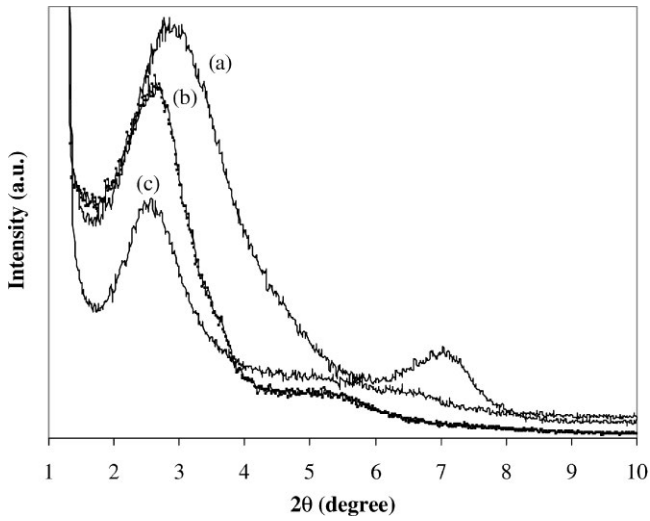

Figure 2.
X-Ray diffraction patterns of a) organoclays, b) masterbatch of PPMA/clay = 3 and c) nanocomposites at $\Phi_v = 0.5\%$.

TEM image of the layered organoclay particles in the PP matrix. A mixed intercalated/Exfoliated microstructure can be noted from the figure. It is clearly observed that silicate layers are mostly exfoliated in the PP phase with some remaining stacks of nanoclay platelets after the mixing steps. The X-ray diffraction results of the nanoclays, master batch (PPMA/nanoclay = 3), and PP nanocomposite prepared with 0.5% (volumic) of nanoclay are illustrated in Figure 2. It is observed that the diffraction peak corresponding to the (001) plane of the nanoclay appears at 2.9°, while the diffraction peak of the master batch appears at a lower angle ($2\theta = 2.75°$, d = 32.10 Å) than that of the nanoclay, indicating an increase in the interlayer distance of the silicates. The interlayer distance of the PP nanocomposite prepared based on 0.5% of clay is about 33.10 Å, larger than the original interlayer spacing of Cloisite 15A and the master batch. It should be noted that the intensity of the diffraction peak in the PP nanocomposite decreases in comparison with the nanoclay and master batch. The decrease in intensity of peaks indicates that the stacks of layered silicates become more exfoliated (Gopakumar et al., 2002); hence, the PP nanocomposite yields more exfoliated structure The melt state rheological properties of nanocomposites were measured using an ARES TA Instrument at the startup of shear flows at 180 °C and under nitrogen flow. A 25 mm parallel plate geometry was used for all measurements on disk samples of nanocomposite prepared by compression molding.

Modeling

To model the internal microstructure of the nanocomposites, two second order three by three tensors are used as state variables to represent the orientation of the particles and extension of the macromolecules. Starting from the description level of kinetic theory, the internal structure state variables on this level are the configuration distribution functions $\Psi(R)$ and $\psi(P)$ denoted for the polymer and for the ellipsoid particles, respectively. R and P are vectors denoting the end to end vector of polymer chains and the spheroids. The distribution functions should also satisfy the normalization conditions defined as:

$$\int \Psi(R)\, dR = 1 \tag{1}$$

$$\int \psi(P)\, dP = 1 \tag{2}$$

We introduce the second order tensor C to describe the extension of polymer chains. In the distribution function space, it can be defined as:

$$C_{ij} = \int R_i R_j \Psi(R)\, dR \tag{3}$$

Throughout this paper, we denote the clay layers as rigid and axi-symmetric oblate particles, with a unit vector P perpendicular to its surface. Therefore, the axis of the disk can be used to describe its orientation according to Figure 3. A group of ellipsoid particles can be represented by a probability distribution function $\psi(P)$, defined as the probability of a particle being aligned within an angular range dP of the direction P is equal to $\psi(P)dP$. As a result, the components of orientation tensor which is the second moment of orientation vector P are expressed as follows:

$$A_{ij} = \int \psi(P)\, P_i P_j dP \tag{4}$$

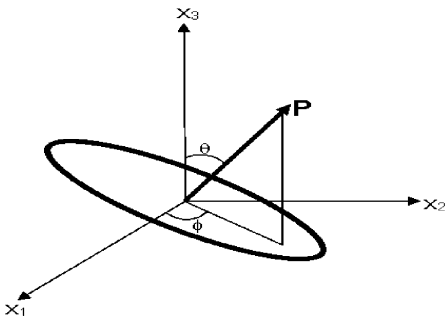

Figure 3.
Schematic of a oblate particle described by the orientation vector P.

Moreover, trace of the orientation tensor A is restricted constant since the particles are assumed to be rigid and inextensible:

$$\mathrm{tr\,A} = 1 \tag{5}$$

Assuming the particles are evenly dispersed in the polymer, the components of the orientation tensor are not varied with the spatial position and only change with time. Thus, from now on we can suppose any information on the particles during the flow is represented by the orientation tensor A.

To derive the time evolution equations for tensors C and A, we use the time evolution equations for the polymer and for the ellipsoid particles derived in details in a previous paper [see reference [6]] as follows:

$$\frac{\mathrm{dC_{ij}}}{\mathrm{dt}} = -\frac{1}{2}\mathrm{C_{jk}}\omega_{\mathrm{ik}} - \frac{1}{2}\mathrm{C_{ik}}\omega_{\mathrm{jk}} + \frac{1}{2}(\mathrm{C_{jk}}\dot{\gamma}_{\mathrm{ik}} + \mathrm{C_{ik}}\dot{\gamma}_{\mathrm{jk}}) - \frac{\partial \Xi}{\partial \varphi_{\mathrm{C_{ij}}}} \tag{6}$$

$$\frac{\mathrm{dA_{ij}}}{\mathrm{dt}} = -\frac{1}{2}\mathrm{A_{jk}}\omega_{\mathrm{ik}} - \frac{1}{2}\mathrm{A_{ik}}\omega_{\mathrm{jk}} - \frac{1}{2}\lambda\,(-\mathrm{A_{ilkl}}\dot{\gamma}_{\mathrm{jk}} - \mathrm{A_{jlkl}}\dot{\gamma}_{\mathrm{ik}} + \mathrm{A_{ilkj}}\dot{\gamma}_{\mathrm{lk}} + \mathrm{A_{jlki}}\dot{\gamma}_{\mathrm{lk}}) - \frac{\partial \Xi}{\partial \varphi_{\mathrm{A_{ij}}}} \tag{7}$$

where λ is a shape factor $\lambda = \frac{(l/d)^2-1}{(l/d)^2+1}$ (l and d denote the spheroids thickness and diameter) and ω_{ij} and $\dot{\gamma}_{ij}$ represent the vorticity and rate of deformation tensors, respectively:

$$\omega_{ij} = \frac{\partial u_j}{\partial x_i} - \frac{\partial u_i}{\partial x_j}; \quad \dot{\gamma}_{ij} = \frac{\partial u_j}{\partial x_i} + \frac{\partial u_i}{\partial x_j} \tag{8}$$

Note that the last term in the right hand side of equation 6 and 7 are dissipation terms and are to be expressed by the derivatives of free energy with respect to tensors C and A. The fourth order tensor orientation tensor a_{ijkl} defined as: $\mathrm{A_{ijkl}} = \int \psi(\mathrm{P})\,\mathrm{P_iP_jP_kP_l dP}$ is to be expressed by the second order orientation tensor using the closure approximation methods. We use the orthotropic closure approximation ORT developed by Cintra and Tuckern.[8]

The overall free energy of the suspensions of ellipsoidal particles in the viscoelastic fluids can be formulated by tensors C and A, provided the terms influencing the rheology as follows [Rajabian et al., 6]:

$$\begin{aligned}\phi(\mathrm{u,A,C}) = \int \mathrm{dr}\frac{\mathrm{u_j u_j}}{2\rho} - \mathrm{n_p\,HR_0^2\ln(1-trC)} \\ - \frac{\mathrm{k_B T}}{2}[\mathrm{n_m ln\ det\,C + n_p\ln det\,A} \\ -2\,\mathrm{B_{pm}\,n_p n_m\,(tra\,trC - trAC)} \\ -2\,\mathrm{B_{pp}\,n_p^2\,((trA)^2 - trAA)}]\end{aligned} \tag{9}$$

where the first term represents the total kinetic energy of the suspension, the second term associated with the FENE-P type dumbbells, and the terms inside the bracket are related to the entropy due to contributions from the macromolecular chains, ellipsoidal particles, the macromolecule-particles and particle-particle interactions. The particle-macromolecule and particle-particle interaction parameters denoted by $\mathrm{B_{pm}}$ and $\mathrm{B_{pp}}$ in Equation 9 are phenomenological parameters that signify the extent of the interactions between the particles and the polymer. The dissipation potential Ξ is a function of free energy derivatives with respect to the conformation tensors ϕ_A and ϕ_c (Rajabian et al. 2005).

$$\Xi = \begin{pmatrix} \phi_{\mathrm{A_{ik}}} - \frac{1}{3}\mathrm{tr}\phi_{\mathrm{A}}\delta_{\mathrm{ik}} & \phi_{\mathrm{c_{ik}}} \end{pmatrix} \cdot \begin{pmatrix} (\partial_{\mathrm{r}}\phi_{\mathrm{u_s}}\partial_{\mathrm{s}}\phi_{\mathrm{u_r}})^{\frac{1}{2}}\Lambda_2\mathrm{A_{kl}} & 0 \\ 0 & \Lambda_1\mathrm{C_{kl}} \end{pmatrix} \cdot \begin{pmatrix} \phi_{\mathrm{A_{li}}} - \frac{1}{3}\mathrm{tr}\phi_{\mathrm{A}}\delta_{\mathrm{li}} \\ \phi_{\mathrm{c_{li}}} \end{pmatrix} \tag{10}$$

Combining the dissipation terms in the governing equations for the conformation and orientation tensors (equation 6 and 7) provides us with the following expressions for the time evolution equations of tensors C and A:

$$\frac{\mathrm{dC_{ij}}}{\mathrm{dt}} = -\frac{1}{2}\mathrm{C_{jk}}\omega_{\mathrm{ik}} - \frac{1}{2}\mathrm{C_{ik}}\omega_{\mathrm{jk}} + \frac{1}{2}(\mathrm{C_{jk}}\dot{\gamma}_{\mathrm{ik}} + \mathrm{C_{ik}}\dot{\gamma}_{\mathrm{jk}}) - \Lambda_1\,(\phi_{\mathrm{C_{ki}}}\mathrm{C_{kj}} - \phi_{\mathrm{C_{kj}}}\mathrm{C_{ki}}) \tag{11}$$

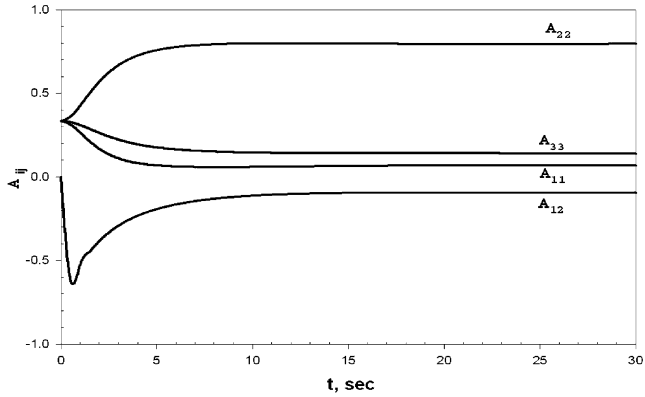

Figure 4.
Orientation tensor components in a simple shear experiment, $\dot{\gamma} = 1\ s^{-1}$, L = 1 nm, d = 100 nm, $\Lambda_1 = 2 \times 10^{-6}$, $\Lambda_2 = 4 \times 10^{-5}$, b = 2.5, Bpp = Bpm = 0.

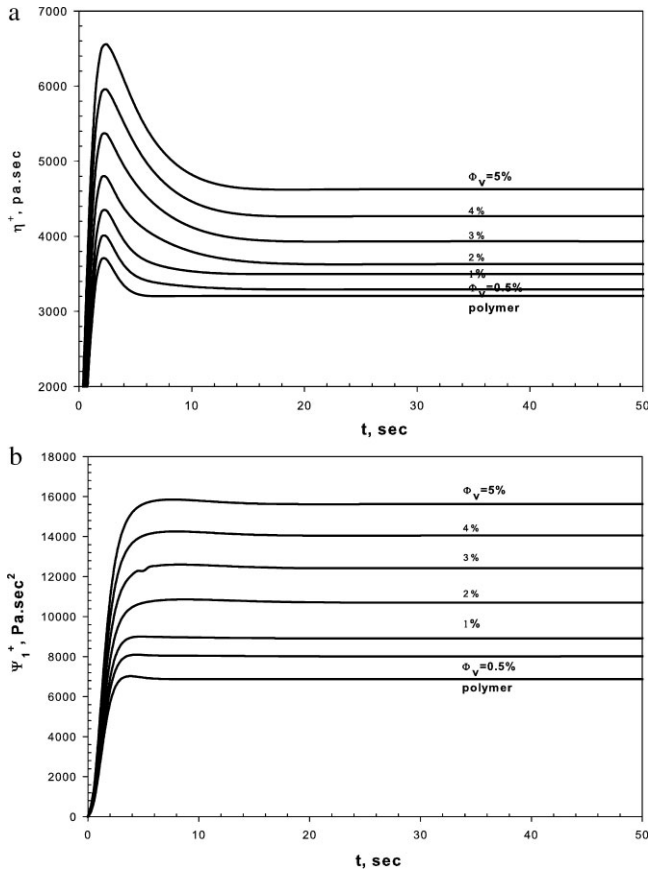

Figure 5.
a. Effects of particle loadings on startup shear viscosity of nanocomposites, L = 1 nm, d = 100 nm, $\Lambda_1 = 2 \times 10^{-6}$, $\Lambda_2 = 4 \times 10^{-5}$, b = 2.5, Bpp = Bpm = 0. b. Effects of particle loadings on transient first normal stress difference coefficient of nanocomposites, $\dot{\gamma} = 1\ s^{-1}$, L = 1 nm, d = 100 nm, $\Lambda_1 = 2 \times 10^{-6}$, $\Lambda_2 = 4 \times 10^{-5}$, b = 2.5, Bpp = Bpm = 0.

$$\frac{dA_{ij}}{dt} = -\frac{1}{2}A_{jk}\omega_{ik} - \frac{1}{2}A_{ik}\omega_{jk} - \frac{1}{2}\lambda\left(-A_{ilkl}\dot{\gamma}_{jk} - A_{jlkl}\dot{\gamma}_{ik} + A_{ilkj}\dot{\gamma}_{lk} + A_{jlki}\dot{\gamma}_{lk}\right) - \frac{1}{4}\dot{\gamma}_{lm}\dot{\gamma}_{lm}\Lambda\left(A_{li}\phi_{A_{lj}} + A_{lj}\phi_{A_{li}}\right) + \frac{1}{6}\dot{\gamma}_{lm}\dot{\gamma}_{lm}\Lambda A_{ji}\phi_{A_{kk}} + \frac{1}{3}\delta_{ij}\left(\frac{1}{2}\left(\partial_k\phi_{ul}\partial_l\phi_{uk}\right)^{\frac{1}{2}}\left(\Lambda A_{lk}\phi_{A_{lk}} - \frac{1}{6}\Lambda\phi_{A_{ll}}\right)\right) \quad (12)$$

Note that the extra stress tensor of the suspension is summation of contributions from the polymer and the particles as follows:

$$\tau_{ij} = -2C_{ik}\phi_{C_{kj}} + \frac{1}{2}\lambda\left(\phi_{A_{lk}}A_{lijk} + \phi_{A_{lk}}A_{kijl} - 2\phi_{A_{mi}}A_{mljl}\phi_{A_{lk}}A_{ljik} + \phi_{A_{mi}}A_{mljl} - 2\phi_{A_{mj}}A_{mlil}\right) - \frac{1}{2} \times \frac{\dot{\gamma}_{ij}}{\left(\partial_k\phi_{ul}\partial_l\phi_{uk}\right)^{\frac{1}{2}}}\Lambda_2\left(\phi_{A_{lm}} - \frac{1}{3}\mathrm{tr}\phi A\delta_{lm}\right)A_{mp}\left(\phi_{A_{lp}} - \frac{1}{3}\mathrm{tr}\phi_A\delta_{lp}\right) \quad (13)$$

where the first term represents the contribution of the polymer (FENE-P type) and the following terms are due to the presence of the particles (non-dissipation followed by the dissipation parts).

Results and Discussions

Figure 4 illustrates the predictions for the orientation tensor components. The orientation tensor components change from initially random orientation ($A_{ii} = 1/3$ at $t = 0$) to the preferred direction corresponding to the velocity gradient vector X_2 (we note that A_{22} is larger than A_{11} and A_{33}). The predictions show that the clay layers are aligned with the shear (see Figure 3 which depicts the vector perpendicular to the disk). Further computations prove that the eigenvectors of the orientation tensor are nearly perfectly aligned with the shear plane after a short time. Figure 5a and 5b represent the model prediction for the viscosity and first normal stress difference of the composites. The rheological properties are found sensitive to the applied shear flow. The viscoelastic behavior of nanosized particulate suspensions is dominated by the particles even at

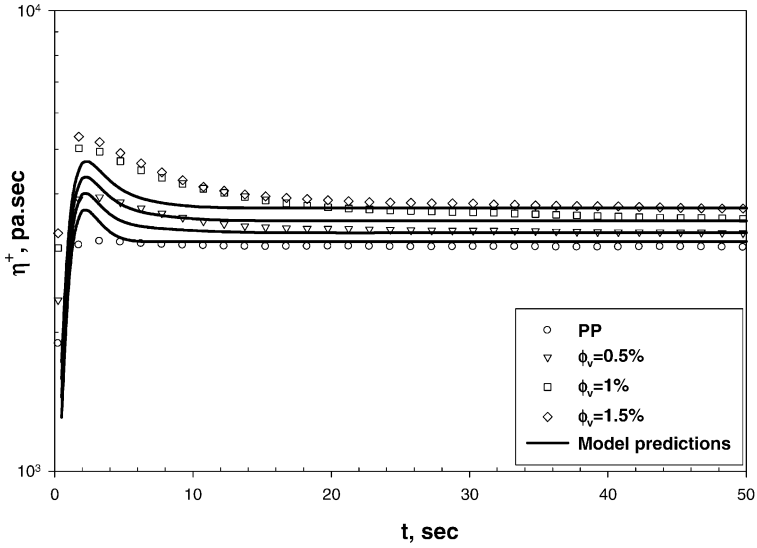

Figure 6.
Experimental results vs. model predictions for startup viscosity of polymer and nanocomposites in simple shear.

low particle loadings. The addition of particle increases both viscosity and first normal stress difference of the nanocomposite. These are due to the fact that a great number of particles are contained in the fluid, thus interacting with the fluid and with each other. Figure 5a shows that the steady state value of viscosity increases with particle contents. One can notice from Figure 4 that after the overshoot the particles are significantly aligned in the direction that is parallel to the shear axis. The stationary value of the normal stress difference coefficient is also increased with particle loadings.

Figure 6 shows the experimental results for the startup viscosity at the three different clay contents. The addition of clay particles to the polymer increases viscous dissipation with an overshoot attributed to the orientation of a major part of clay particles. Reasonable agreement is observed between the model predictions shown by the solid lines with the experimental results even though the peak of viscosity is under-predicted with respect to the measurements.

Conclusion

It has been shown that nanocomposites of organoclays in a thermoplastic matrix, i.e. polypropylene with the mixed exfoliated/intercalated microstructure were produced and their rheological properties under simple shear flow were investigated. A rheological model on the mesoscopic level of description to study the motion of a group of ellipsoid particles which uses the particle orientation and polymer conformation tensors has been presented to predict the orientation state of particles and the flow characteristics of nano-sized disk shape particles in a viscoelastic fluid. The hydrodynamic interactions and particle-particle effects have been considered in the governing equations and were found to alter both viscous dissipation and normal stress difference of suspensions. The motion of particles was successfully predicted by this model and accordingly the orientation process of layered particles with the applied shear was studied. The startup viscosity results show an overshoot which its magnitude increases with particle loadings. Model calculations demonstrate a great number of particles are oriented in the shear direction after the overshoot.

[1] M. Rajabian, G. Naderi, M. H. Beheshty, P. G. Lafleur, C. Dubois, P. J. Carreau, *Int. Polym. Process.* **2008**, *XXIII*, 110.
[2] M. Rajabian, M. H. Beheshty, *Polymer Composites.* **2008**, in Press.
[3] W. Letwimolnum, B. Vergnes, G. Ausias, P. J. Carreau, *J. Non-Newtonian Fluid Mech.* **2007**, *141*, 167.
[4] G. Naderi, P. G. Lafleur, C. Dubois, *Polym. Eng. Sci.* **2007**, *47*, 207.
[5] M. Rajabian, C. Dubois, M. Grmela, P. J. Carreau, *Rheol. Acta* **2008**, *47*, 701–717.
[6] M. Rajabian, C. Dubois, M. Grmela, *Rheol. Acta* **2005**, *44*, 521–535.
[7] R. B. Bird, R. C. Armstrong, O. Hassager, "*Dynamics of polymeric liquids*", Vol. 1, second ed., John Wiley, New York **1987**.
[8] J. S. Cintra, C. L. Tucker, *J. Rheol.* **1995**, *39*, 1095.
[9] T. G. Gopakumar, J. A. Lee, M. Kontopoulou, J. S. Parent, *Polymer* **2002**, *43*, 5483.
[10] M. Grmela, H. C. Ottinger, *Phys. Rev. E* **1997**, *55*, 6620.
[11] M. Rajabian, C. Dubois, *Polym. Comp.* **2006**, *27*, 129.
[12] J. Ren, B. F. Casa nueva, C. A. Mitchell, R. Krishnamoorti, *Macromolecules* **2003**, *36*, 4188–4194.

